

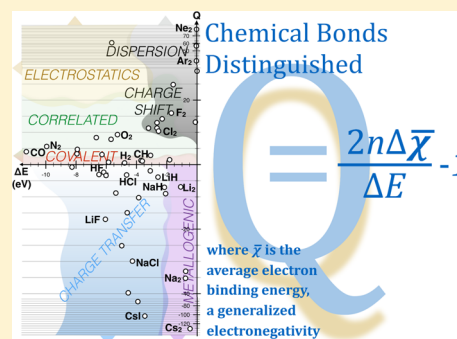
Distinguishing Bonds

Martin Rahm* and Roald Hoffmann

Chemistry and Chemical Biology, Baker Laboratory, Cornell University, Ithaca, New York 14853, United States

S Supporting Information

ABSTRACT: The energy change per electron in a chemical or physical transformation, $\Delta E/n$, may be expressed as $\Delta\bar{\chi} + \Delta(V_{\text{NN}} + \omega)/n$, where $\Delta\bar{\chi}$ is the average electron binding energy, a generalized electronegativity, ΔV_{NN} is the change in nuclear repulsions, and $\Delta\omega$ is the change in multielectron interactions in the process considered. The last term can be obtained by the difference from experimental or theoretical estimates of the first terms. Previously obtained consequences of this energy partitioning are extended here to a different analysis of bonding in a great variety of diatomics, including more or less polar ones. Arguments are presented for associating the average change in electron binding energy with covalence, and the change in multielectron interactions with electron transfer, either to, out, or within a molecule. A new descriptor Q , essentially the scaled difference between the $\Delta\bar{\chi}$ and $\Delta(V_{\text{NN}} + \omega)/n$ terms, when plotted versus the bond energy, separates nicely a wide variety of bonding types, covalent, covalent but more correlated, polar and increasingly ionic, metallogenic, electrostatic, charge-shift bonds, and dispersion interactions. Also, Q itself shows a set of interesting relations with the correlation energy of a bond.



INTRODUCTION

This work is the second in a series¹ developing a different approach to rationalizing and analyzing chemistry. The previous paper began, following the work of L. C. Allen,^{2–5} by considering the average electron binding energy of all electrons, a quantity that we termed $\bar{\chi}$, a generalized electronegativity. Here, we continue our investigation of a new kind of energy decomposition analysis based on terms that are attainable from experimental and theoretical methods alike.

The energy partitioning that comes out of the definition of $\bar{\chi}$ involves in a natural way two other terms: ω , a negative of multielectron interactions, and V_{NN} , a more straightforward sum of nuclear repulsions. We will refresh the exact definition of these terms below. An important point in our theory, that explicit quantification of multielectron interactions can be gained purely from accurate experimental data for small molecules, was illustrated in the previous article. Herein, we apply this energy partitioning analysis to bond formation in diatomics. Using its framework, we will show how familiar classes of bonding motifs appear as a natural consequence of the analysis. Chemical concepts such as covalence, ionicity, and highly correlated situations can be investigated both from calculations and from experiment.

First, quite some background is required, and we ask the reader to bear with us.

WHERE IT BEGINS: THE AVERAGE ELECTRON BINDING ENERGY, $\bar{\chi}$

The average binding energy of a collection of electrons ($\bar{\chi}$) is a property of any assembly of electrons in atoms, molecules, or extended materials. One approximation to $\bar{\chi}$ is as an average of ionization potentials:

$$\bar{\chi} = \frac{\sum_i \varepsilon_i}{n} \quad (1)$$

where ε_i is the energy corresponding to the vertical (Franck–Condon) emission of one electron i into vacuum, with zero kinetic energy, and n is the total number of electrons. For extended structures in one-, two-, or three-dimensions, $\bar{\chi}$ can similarly be obtained from the density of states (DOS).¹

It is important to stress that the definition of $\bar{\chi}$ does not necessitate a “single particle picture” because any collection of electrons in a specified electronic state collectively has an average binding energy, which is characteristic of the system. Significant degrees of entanglement (or correlation) of the electrons do not change this. Estimates to $\bar{\chi}$ from experiment are possible;¹ however, the interpretation of photoelectron spectra can, for instance, be problematic when ionization arises from strongly coupled states.^{6–8} As will be discussed, $\bar{\chi}$ can be approached and approximated using several levels of theory, including one- and multideterminant self-consistent field theories, and density functional theory. As one moves beyond single-reference descriptions, the interpretation of $\bar{\chi}$ in terms of ionization potentials becomes approximate, but its interpretation as an inherent average of electron binding energies remains.

$\bar{\chi}$ also appears in the theoretical framework of moments of the electron distribution, pursued by Pettifor, Burdett, and Lee, for describing factors behind solid-state structure.^{9–12} Politzer, Murray, and co-workers have investigated the average local ionization energy, essentially a spatially distributed equivalence

Received: November 28, 2015

Published: February 24, 2016

of $\bar{\chi}$, on isosurfaces of constant electron density, within the contexts of molecular reactivity,^{13–15} electronegativity,¹⁶ polarizability,^{17,18} and other properties.¹³

As we showed in our previous paper, and as L.C. Allen suggested, the average binding energy $\bar{\chi}$ is related to the well-known idea of electronegativity. There exist, of course, numerous definitions of electronegativity.^{2,16,19–34} The concept was first conceived by Pauling, who termed it as “the power of an atom to attract electrons to itself.” He then chose to quantify this notion by defining it on the basis of bond dissociation energies.¹⁹

In the first part in this series, we demonstrated how $\bar{\chi}$ could be obtained for individual atoms, molecules, and extended systems alike. This was done using both theoretical calculations as well as accurate experimental data. $\bar{\chi}$ correlates well with other scales of electronegativity, but only within periods of the periodic table. $\bar{\chi}$ deviates from traditional electronegativity scales in one important aspect; as elements grow heavier, down the periodic table, the absolute $\bar{\chi}$ -values increase as more electrons are bound. This is not the case for traditional electronegativity, which focuses, in different ways, on the valence electrons; there are advantages and disadvantages to this definition, which we outlined before. Fortunately, this difference in absolute values does not matter, for our analysis focuses on relative measures, that is, $\Delta\bar{\chi}$. In a relative setting, $\Delta\bar{\chi}$ values, whether computed from valence-only or all-electron estimates, are often (but not always) similar. However, we caution that this assumption can be qualitatively incorrect, especially for heavier elements where a large number of “core” levels may change their energies (in different directions) in the course of chemical transformations.

■ AN EXPERIMENTAL AND THEORETICAL ENERGY DECOMPOSITION ANALYSIS

The basis for the analysis that grows out of the definition of $\bar{\chi}$ is as follows: When one ignores rotational, vibrational, and translational contributions, the total energy per electron (E/n) of any system can be related to $\bar{\chi}$ as

$$E/n = \bar{\chi} + (V_{\text{NN}} + \omega)/n \quad (2)$$

Here, n is the total number of electrons, $\bar{\chi}$ is the average binding energy of said electrons (obtained from experiment or theory), and V_{NN}/n is the nuclear–nuclear repulsion energy, per electron. V_{NN} is a direct consequence of the relative positions of all nuclei, that is, of molecular structure. The latter can, of course, be obtained by, for instance, X-ray diffraction, microwave spectroscopy, or from quantum chemical calculations. Finally, ω is a key feature of this analysis. It represents multielectron interactions. This quantity is the only term of eq 2 that cannot be directly experimentally measured over a reaction. Instead, as previously detailed, and as we will show below, it can be indirectly inferred, quantitatively so, following measurement of all other components of eq 2: ΔE , $\Delta\bar{\chi}$, and ΔV_{NN} .

■ DO WE NEED ANOTHER ENERGY DECOMPOSITION ANALYSIS?

Ever since the advent of quantum chemistry, people have tried to analyze electronic structure through a variety of approaches.^{35,36} There exist a variety of methods specifically focused on decomposing the total energy (E), or the relative energy change in a reaction (ΔE), which can be referred to as

energy decomposition analyses, or EDAs. A long but still not exhaustive list includes the schemes of Kitaura and Morokuma,³⁷ Ziegler and Rauk,³⁸ the Constrained Space Orbital Variation (CSOV) method of Bagus and Illas,^{39,40} the Reduced Variational Self-Consistent Field (RVS-SCF) method of Stevens and Fink,⁴¹ the Natural Energy Decomposition Analysis (NEDA) of Glendening and Streitwieser,^{42–44} in turn based on the Natural Bond Orbital (NBO) method (which is not an energy decomposing method),^{45,46} the Self-Consistent Charge and Configuration Method for Subsystems (SCCCMS) of Korchowiec and Uchimaru,⁴⁷ the method of Mayer,⁴⁸ the Atomic Resolution of Identity approach of Mayer and Hamza,⁴⁹ the symmetry-adapted perturbation theory (SAPT) method,^{50–52} the approaches of Vyboishchikov and Salvador,⁵³ Frenking and co-workers,^{54,55} the QTAIM⁵⁶ and DFT-based Molecular Energy Decomposition Scheme of Francisco et al.,⁵⁷ the DFT-based EDA by Wu, Ayers, and Zhang,^{58,59} the Natural Atomic Orbital based method of Baba et al.,^{60,61} the steric analysis by Liu,⁶² the Absolutely Localized Molecular Orbitals (ALMO) EDA of Head-Gordon and co-workers,^{63,64} and the block-localized wave function-based energy decomposition (BLW-ED) analysis of Mo et al.⁶⁵

The details of these elegant and useful approaches are not trivial, yet they share one thing in common; they all require a quantum mechanical calculation to approximate a wave function (or a density), which subsequently can be analyzed. Our $\bar{\chi}$ -based analysis might not offer as much intricate detail (in the number of contributing energy terms) as some of the above-mentioned methods. However, with it we have the option to rely on experimental data, or to intermix the use of experimental and theoretical sources of data. One is free to approximate the three required components, ΔE , $\Delta\bar{\chi}$, and ΔV_{NN} , as best as one can, using any experimental methodology or theoretical framework deemed most suitable. Of course, this freedom does not absolve one from concern about the accuracy and precision of the numbers used, be they experimental or theoretical.

We have in this work used a hybrid approach: ΔE and ΔV_{NN} are experimentally determined. We thus incorporate difficult correlation effects experimentally, while minimizing ambiguity in the ΔV_{NN} -term. The remaining term, $\Delta\bar{\chi}$, capturing the average behavior of the individual electrons, is here obtained from molecular orbital theory calculations. As mentioned above, below, and in our previous work, there are many other ways of estimating this term.

Let us begin with a recap of the interpretation of $\bar{\chi}$ and ω .

■ UNDERSTANDING $\bar{\chi}$ AND ω BY EXPRESSING THEM WITHIN HARTREE–FOCK, KOHN–SHAM DENSITY FUNCTIONAL THEORY, AND MULTIREFERENCE WAVE FUNCTIONS

To gain an appreciation for the meaning of ω , let us express the total energy in several ways. One first and mean-field approximation to $\bar{\chi}$ is the average energy of all occupied Hartree–Fock molecular orbitals, which by themselves, via Koopmans’ theorem, approximate single electron vertical ionization potentials.⁶⁶ In closed-shell Hartree–Fock theory, $\bar{\chi}_{\text{HF}}$ is defined as

$$\bar{\chi}_{\text{HF}} = n^{-1} \sum_{i=1}^n \varepsilon_i = n^{-1} \sum_{i=1}^n \left(\left\langle \phi_i \left| -\frac{1}{2} \nabla_i^2 - \sum_{A=1}^M \frac{Z_A}{r_{Ai}} \right| \phi_i \right\rangle + \sum_{i<j} (2J_{ij} - K_{ij}) \right), \quad (3)$$

where n is the total number of electrons, ε_i is here the eigenvalue of ϕ_i , which is the spin-orbital of electron i , ∇_i^2 is the one-electron kinetic energy operator, $\sum_{A=1}^M \frac{Z_A}{r_{Ai}}$ is the electron–nuclear attraction operator between each electron i and nuclei A , for M number of nuclei, and J_{ij} and K_{ij} are the matrix elements of the Coulomb and exchange operators, respectively.⁶⁶ The total energy E_{HF} within Hartree–Fock theory can then be expressed by eq 4.

$$E_{\text{HF}} = n\bar{\chi}_{\text{HF}} + V_{\text{NN}} - \underbrace{\frac{1}{2} \sum_{i<j} (2J_{ij} - K_{ij})}_{\omega}. \quad (4)$$

ω clearly represents multiple-electron interactions, precisely expressed in terms of the same Coulomb and Exchange operators that enter $\bar{\chi}_{\text{HF}}$. Importantly ω , as defined by eq 4, includes the negative of the electron–electron repulsion and of the positive exchange and correlation energy. This seemingly unphysical reversal of sign of the electron–electron repulsion is a consequence of expressing the total energy as a function of $\bar{\chi}$ (eq 2), and is necessary to avoid “double counting” the electron–electron interactions. Thus, when $\Delta\omega/n$ is negative over a reaction, electron–electron interactions are actually increased, and vice versa.

The expression analogous to eq 4 in Kohn–Sham density functional theory (which, in principle, is an exact theory)^{67–70} can be written such that

$$E_{\text{KS}} = n\bar{\chi}_{\text{KS}} + V_{\text{NN}} - \underbrace{V_{\text{ee}}(\rho) + E_{\text{XC}}(\rho) - \int \frac{\delta E_{\text{XC}}(\rho)}{\delta \rho(r)} \rho(r) dr}_{\omega}, \quad (5)$$

where $V_{\text{ee}}(\rho)$ is the classical electron–electron Coulomb repulsion energy, E_{XC} is the exchange–correlation energy, $\rho(r)$ is the electron density, and the last term is the exchange–correlation potential.

One straightforward approach to $\bar{\chi}$ within KS-DFT is to estimate it from orbital energies computed using range-separated DFT.^{71–73} In this manner, one limits the self-interaction error inherent in DFT by compensating with exact Hartree–Fock exchange at longer distances. This approach typically provides good estimates to (especially) the valence electron binding energies, which are those energies that vary most over a chemical reaction. For this reason, and due to error cancellations, estimates of $\Delta\bar{\chi}$ become considerably more reliable. In this work, we will use the LC-BLYP functional for this purpose. The physical meaning of DFT orbital energies has been extensively discussed,^{74–80} and within DFT, several other technical approaches can be taken to approximate more accurate single electron binding energies.^{75,76}

Thanks to work by Ryabinkin and Staroverov,⁸¹ it is possible to also rigorously define $\bar{\chi}$ more generally without the explicit need for orbitals:

$$\bar{\chi}_{\text{gen}} = n^{-1} \int \left(\tau_{\text{L}}(\mathbf{r}) + v(\mathbf{r})\rho(\mathbf{r}) + 2 \int \frac{P(\mathbf{r}, \mathbf{r}_2)}{|\mathbf{r} - \mathbf{r}_2|} d\mathbf{r}_2 \right) d\mathbf{r}, \quad (6)$$

where $\tau_{\text{L}}(\mathbf{r})$ is the Laplacian form of the kinetic-energy density, $v(\mathbf{r})$ is the external potential, $\rho(\mathbf{r})$ is the electron density, and $P(\mathbf{r}, \mathbf{r}_2)$ is the diagonal of the two-electron reduced density matrix, all of which can be extracted from any single- or multireference wave function. Within this coordinate representation, the analogous expression to eq 4 then reads as

$$E_{\text{gen}} = \bar{\chi}_{\text{gen}} + V_{\text{NN}} - \underbrace{\int \frac{P(\mathbf{r}, \mathbf{r}_2)}{|\mathbf{r} - \mathbf{r}_2|} d\mathbf{r}_2}_{\omega}. \quad (7)$$

BOND FORMATION

Our first article in this series included, among other things, the analysis of the following simple exoergic reactions, from experimental data:

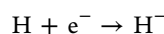
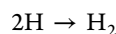


Table 1 shows the various energy components of these two reactions.

Table 1. Experimental Energy Partitioning of Two Simple Reactions^a

	$\Delta E/n$	$\Delta\bar{\chi}$	$\Delta V_{\text{NN}}/n$	$\Delta\omega/n$
$2\text{H} \rightarrow \text{H}_2$	−2.396	−1.828	9.716	−10.285
$\text{H} + \text{e}^- \rightarrow \text{H}^-$	−0.377	6.045	0.000	−6.422

^aAll energies are given in eV e^{−1}.

Both reactions are exoergic, but the components of the total energy combine in a very different way to give the final result of a negative ΔE . In the first reaction, we have a positive $\Delta V_{\text{NN}}/n$ and a negative $\Delta\omega/n$, as expected. The two nearly cancel and the negative ΔE comes primarily from the negative $\Delta\bar{\chi}$, with a secondary contribution from $\Delta\omega/n$. This is what we usually expect of bond formation, that it is driven by a lowering of orbital energies. The physical picture is an increase in the average binding energy of electrons as the bond forms; we will loosely use the terms “orbital” and “average binding energy” interchangeably. This is to ease understanding, and is not meant to imply that orbitals are experimental observables. They are the result of a mean field theory, and their average energies represent an approximation to $\bar{\chi}$.

By a classification scheme laid out in the previous publication, this first reaction is “nuclear-resisted”. As the naming implies, this means that the exothermic bond formation process is resisted only by nuclear–nuclear repulsion ($\Delta V_{\text{NN}}/n$ -term in eq 2). The reaction is energetically favored both by the lowering of orbital energies ($\Delta\bar{\chi} < 0$) and by multielectron interactions ($\Delta\omega < 0$).

The second reaction, $\text{H} + \text{e}^- \rightarrow \text{H}^-$, departs fundamentally from this paradigm. This example of electron attachment shows how a simple exoergic process can be favored only by multielectron interactions ($\Delta\omega < 0$), while actually resisted by orbital energies ($\Delta\bar{\chi} > 0$). By the classification scheme laid out in the previous article, we refer to such reactions as “multielectron-favored”.

The reader will note that the “favored” and “resisted” suffixes do not relate to the exo- or endoenergetic character of the reaction. So H_2 formation and electron attachment to H are both exothermic, while the first is termed nuclear-resisted and the second multielectron-favored. The “favored” and “resisted” labels refer only to the single factor (among $\Delta\bar{\chi}$, ΔV_{NN} , and $\Delta\omega$) that differs, going against the other two. A reason for this focus will emerge in time.

We will demonstrate that both the nuclear and the multielectron typologies both resurface when studying bond making and breaking in a range of diatomics. It will emerge that for reactions classified as nuclear-resisted, we can use traditional electronegativity arguments (here reinterpreted as the average electron binding energy) to rationalize energetic preferences, whereas for multielectron-favored reactions such quick and intuitive arguments will inevitably fail us. In one way, the border between the two represents a sort of limit, a limit that will help us in an effort to assign a measure to the chemical concepts of “covalence” and “ionicity”.

The obvious path ahead takes us to the homonuclear diatomics, which include bonds of very different strength and nature. Let us begin with an in-depth analysis of one of the more unusual cases, the weak bond of Li_2 .

■ AN EXAMPLE: DILITHIUM, Li_2

The lithium diatomic is, of course, real, albeit not very stable thermodynamically, nor persistent kinetically. The Li–Li distance in Li_2 has been determined as 2.67 Å, which tells us that the nuclear repulsion energy change in $2Li \rightarrow Li_2$ is relatively small, +8.08 eV e^{-1} (Figure 1). The heat of formation

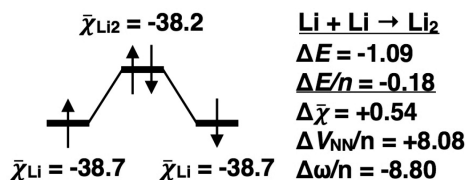


Figure 1. In the exothermic formation of Li_2 from Li atoms, the average electron binding energy is increased.

(ΔH_f^0) of atomic Li and Li_2 has been measured to be 1.65 and 2.24 eV, respectively. The reaction $2Li \rightarrow Li_2$ is, in other words, exothermic by 1.064 eV. The vibrational contribution to the total energy, ΔE_{ZPE} , is negligible, ~ 22 meV, making our best estimate of the bonding energy, $\Delta E = -1.064 - 0.022 = -1.09$ eV for $2Li \rightarrow Li_2$. We can use experimental electron binding energies, and calculate $\bar{\chi}$ for Li using eq 1, $\bar{\chi} = (2^* - 55.35 + (-5.39))/3 = -38.70$ eV e^{-1} . However, because experimental data on Li_2 are scarce, we turn instead to quantum mechanical calculations. In place of photoelectron spectroscopy measurements, we apply LC-DFT calculations on the $2Li \rightarrow Li_2$ reaction, and predict $\Delta\bar{\chi}$ to be +0.54 eV e^{-1} . This, in turn, allows the calculation of $\Delta\omega/n = -8.80$ eV e^{-1} , and $\Delta(V_{NN} + \omega)/n = -0.71$ eV e^{-1} , via eq 2.

The positive value of $\Delta\bar{\chi}$ for the formation of such a simple diatomic, in an exoergic reaction, should raise an eyebrow. The unexpected increase in $\Delta\bar{\chi}$ in the course of the $2Li \rightarrow Li_2$ reaction can be traced to the $1\sigma_g$ and $2\sigma_g$ molecular orbitals, which, upon formation, increase in energy relative to the 1s and 2s atomic orbitals of Li. This effect was first noted by Harrison and Lawson.⁸² Whereas the accuracy of DFT functionals in estimating $\bar{\chi}$ is quite good for larger systems, it is less so for the light atoms H and Li. However, this “anomalous” orbital effect cannot be attributed to DFT’s inherent problem of self-interaction error, because a near identical value for the $2Li \rightarrow Li_2$ reaction is obtained also with Hartree–Fock theory (+0.58 eV e^{-1}). One hand-wavy rationalization for this effect in Li_2 is that exchange (same-spin) repulsion occurs due to overlap of s-orbitals of different principal quantum number (different shell), positioned on adjacent atoms.

So what holds Li_2 together, if $\Delta\bar{\chi}$ is positive? It is $\Delta\omega/n$, the change in multielectron interactions, whose magnitude is such (it is negative) that it exceeds $\Delta V_{NN}/n$ by more than the rise in $\Delta\bar{\chi}$. $2Li \rightarrow Li_2$ classifies as a multielectron-favored reaction, a very different situation in forming a bond from H_2 , and one resembling electron attachment to H.

We have seen how H_2 formation is driven by the increase in electron binding energy, while Li_2 bonding is determined by multielectron interactions. What about the other homonuclear diatomics?

Table 2. Examples of Homonuclear Diatomic Bond Formation^a

reaction ^b	d_{exp} ^c [Å]	n [e]	ΔE^c [eV]	$\Delta E/n$ [eV e^{-1}]	$\Delta\bar{\chi}^d$ [eV e^{-1}]	$\Delta V_{NN}/n^c$ [eV e^{-1}]	$\Delta\omega/n$ [eV e^{-1}]	$\Delta(V_{NN} + \omega)/n$ [eV e^{-1}]
$2^2H \rightarrow H_2$	0.741	2	-4.792	-2.396	-1.828 ^d	+9.716	-10.285	-0.568
$2^2Li \rightarrow Li_2$	2.673	6	-1.09	-0.181	+0.54	+8.08	-8.80	-0.72
$2Be \rightarrow Be_2$	2.460	8	-0.11 ^c	-0.014	-0.10	+11.71	-11.62	+0.09
$2^2B \rightarrow ^3B_2$	1.590	10	-3.07	-0.307	-0.59	+22.64	-22.35	+0.29
$2^3C \rightarrow C_2$	1.243	12	-6.29	-0.524	-1.08	+34.75	-34.20	+0.56
$2^4N \rightarrow N_2$	1.098	14	-9.94	-0.710	-2.35	+45.90	-44.26	+1.64
$2^3O \rightarrow ^3O_2$	1.208	16	-5.26	-0.329	-1.70	+47.68	-46.32	+1.37
$2^2F \rightarrow F_2$	1.412	18	-1.70	-0.095	-0.80	+45.89	-45.18	+0.71
$2^2Na \rightarrow Na_2$	3.079	22	-1.81	-0.035	+0.60	+25.72	-26.35	-0.63
$2^2Al \rightarrow ^3Al_2$	2.466	26	-1.81	-0.070	-0.09	+37.96	-37.94	+0.02
$2^2Cl \rightarrow Cl_2$	1.987	34	-2.55	-0.075	-0.43	+61.60	-61.25	+0.35
$2^2Cu \rightarrow Cu_2$	2.220	58	-2.08	-0.036	+0.14	+94.06	-94.21	-0.18
$2^2I \rightarrow I_2$	2.666	106	-1.58	-0.015	-0.19	+143.13	-142.95	+0.18
$2^2Cs \rightarrow Cs_2$	4.470	110	-0.48	-0.004	+0.28	+88.59	-88.87	-0.29

^aThe bond energy is partitioned from an intermixed use of experimental and theoretical data. ^bThe spin multiplicity is singlet, unless otherwise specified. ^cExperimental data from *NIST Chemistry WebBook*. $\Delta E \approx \Delta H^0 - E_{ZPE}$, where $E_{ZPE} = 1/2h \sum \nu_i$. ^dFrom LC-BLYP/avg-cc-pVQZ calculations, except for H and H_2 , where the experimental values of $\bar{\chi}_H = -13.598$ eV and $\bar{\chi}_{H_2} = -15.426$ eV were used. ^e $\Delta E \approx \Delta H^0$ as E_{ZPE} can be presumed small, and no vibrational data are available for Be_2 .

Table 3. Examples of Heteroatomic Diatomic Bond Formation^a

reaction ^b	d_{exp}^c [Å]	dipole ^c [D]	n [e]	ΔE^c [eV]	$\Delta E/n$ [eV e ⁻¹]	$\Delta\bar{\chi}^d$ [eV e ⁻¹]	$\Delta V_{\text{NN}}/n^c$ [eV e ⁻¹]	$\Delta\omega/n$ [eV e ⁻¹]	$\Delta(V_{\text{NN}} + \omega)/n$ [eV e ⁻¹]
Nuclear-Resisted Bonds, $\Delta\bar{\chi} < 0$									
⁴ N + ³ O → ² NO	1.151	0.153	15	-6.66	-0.444	-2.08	+46.72	-45.08	+1.64
³ C + ³ O → CO	1.128	0.112	14	-11.29	-0.806	-2.02	+43.76	-42.54	+1.22
³ C + ² F → ² CF	1.272	0.7 ^{cd}	15	-5.69	-0.379	-1.68	+40.76	-39.46	+1.30
² B + ² F → BF	1.263	1.02 ^f	14	-7.91	-0.565	-1.62	+36.66	-35.61	+1.05
⁴ N + ³ C → ² CN	1.172	1.45	13	-7.95	-0.611	-1.33	+39.70	-38.98	+0.72
⁴ N + ² F → ³ NF	1.317	0.07 ^d	16	-3.21	-0.201	-1.24	+43.05	-42.02	+1.04
² F + ³ O → ² OF	1.32 ^e	0.03 ^d	17	-2.31 ^e	-0.136	-1.03	+45.14	-44.24	+0.90
² F + ² Cl → ClF	1.628	0.88	26	-2.65	-0.102	-0.71	+52.04	-51.43	+0.61
² B + ² H → BH	1.232	1.2	6	-3.62	-0.604	-0.64	+9.74	-9.71	+0.03
³ C + ² H → ² CH	1.120	1.46	7	-3.71	-0.530	-0.61	+11.02	-10.94	+0.08
² B + ⁴ N → ³ BN	1.281	2.4 ^d	12	-5.85	-0.488	-0.43	+32.79	-32.85	-0.06
² B + ³ O → ² BO	1.205	2.6 ^d	13	-8.27	-0.636	-0.08	+36.78	-37.35	-0.56
Multielectron-Favored Bonds, $\Delta\bar{\chi} > 0$									
² Al + ² H → AlH	1.648	0.08 ^d	14	-3.10	-0.221	+0.10	+8.11	-8.44	-0.32
³ Si + ³ S → SiS	1.929	2.1 ^d	30	-6.48	-0.216	+0.22	+55.73	-56.17	-0.44
² H + ² Cl → HCl	1.274	1.109	18	-4.66	-0.259	+0.28	+10.67	-11.21	-0.54
² H + ² F → HF	0.917	1.826	10	-6.17	-0.617	+0.42	+14.14	-15.18	-1.04
² Na + ² H → NaH	1.887	6.6 ^d	12	-2.16	-0.180	+0.54	+6.99	-7.72	-0.72
Be + ² F → ² BeF	1.361	1.2 ^d	13	-6.02	-0.463	+0.55	+29.30	-30.31	-1.01
² Al + ³ S → ² AlS	2.029	4.4 ^d	29	-3.86	-0.133	+0.62	+50.90	-51.65	-0.75
² Li + ² H → LiH	1.596	5.882	4	-2.58	-0.646	+0.93	+6.80	-8.38	-1.57
² Al + ³ O → ² AlO	1.618	4.9 ^d	21	-5.37	-0.256	+1.00	+44.08	-45.33	-1.25
² Cs + ² Cl → CsCl	2.906	10.36	72	-4.55	-0.063	+1.23	+64.34	-65.63	-1.29
² Cs + ² I → CsI	3.315	11.6	108	-3.50	-0.032	+1.65	+117.24	-118.93	-1.68
² K + ² Br → KBr	2.821	10.6	54	-3.96	-0.073	+2.56	+62.86	-65.50	-2.64
Be + ³ O → BeO	1.331	7.0 ^d	12	-4.62	-0.385	+2.68	+28.85	-31.92	-3.06
² Li + ² F → LiF	1.564	6.284	12	-6.06	-0.505	+4.03	+20.72	-25.25	-4.54
² Na + ² F → NaF	1.926	8.123	20	-4.98	-0.249	+3.01	+37.01	-40.27	-3.26
² Na + ² Cl → NaCl	2.361	8.971	28	-4.27	-0.153	+2.21	+40.74	-43.10	-2.36
² H + e ⁻ → H ⁻	0.0	0.0	2	-0.754	-0.377	+6.045 ^b	0.00	-6.422	-6.42

^aThe bond energy is partitioned from an intermixed use of experimental and theoretical data. ^bThe spin multiplicity is singlet, unless otherwise specified. ^cExperimental data from NIST Chemistry WebBook. $\Delta E \approx \Delta H^0 - E_{\text{ZPE}}$, where $E_{\text{ZPE}} = 1/2h \sum \nu_i$. ^dFrom LC-BLYP/aug-cc-pVQZ calculations, except for H, where the experimental value $\bar{\chi} = -13.598$ eV was used. ^eBecause the reported bond length of 1.32 Å for OF is not reliable and the heat of formation has not been reported, we calculated both at the CBS-QB3 level.⁸⁶ A bond distance of 1.351 Å resulted, which does not affect any conclusions. ^fThe dipole moment of 1.02 D for BF (with the negative end on boron) is from ab initio calculations.⁸⁴ The unsigned NIST experimental value of 0.5 D is deemed unreliable.⁸⁵

■ HOMONUCLEAR DIATOMICS

With the exception of Li₂ and other “metallogenic” (we will define this term in time) dimers such as Na₂, Cs₂, and Cu₂, the formation of all investigated homonuclear diatomics from separate ground state atoms follows the H₂ paradigm (Table 2) in that they may all be classified as nuclear-resisted. The values of $\Delta V_{\text{NN}}/n$ and $\Delta\omega/n$ are uniformly large and largely canceling. $\Delta\bar{\chi}$ has the same sign as ΔE , and we can therefore argue that our favorite conceptual tool, the orbital, here averaged in the form of $\bar{\chi}$, governs these reactions’ exothermicity. The combined effect of the binding energy increase or orbital stabilization ($\Delta\bar{\chi}$) can, however, in some cases far exceed $\Delta E/n$.

The total energy change upon nuclear-resisted bond formation should be understood as a balance between a decrease in $\bar{\chi}$ (the stabilization of orbitals) and the repulsive interactions of approaching nuclei, which in turn cause an increase in electron–electron interactions.

Close to one extreme, we have the formation of F₂, where the increased average electron binding energy $\Delta\chi$ is almost equal in magnitude and opposite in sign to the term $\Delta(V_{\text{NN}} + \omega)/n$.

This signifies that the F₂ bond, albeit governed by the $\Delta\chi$ term, also contains significant multielectron-contributions (the interpretation of the $\Delta(V_{\text{NN}} + \omega)/n$ -term will be addressed below). This trend is in qualitative agreement with the reasoning of Shaik, Danovich, Wu, and Hiberty, who have pointed out in their analysis of charge-shift bonding that bonding with “excessive exchange repulsion is typical to electronegative and lone-pair-rich atoms.”⁸³ One curiosity is that the nuclear–nuclear repulsion energies per electron, V_{NN}/n , in N₂ and F₂ are almost identical, only differing by 9 meV e⁻¹. Thus, as nitrogen is transmuted into fluorine, the longer bond length of F₂ compensates nearly perfectly for fluorine’s higher nuclear charge.

■ POLAR BONDS

In Table 3 we see a variety of “polar” heteronuclear diatomic molecules. When they are analyzed with our energy partitioning, these diatomics also partition into two categories, nuclear-resisted and multielectron-favored. In both groups, there are examples of quite polar (as measured by values of

dipole moment) molecules. Yet by and large the multielectron-favored category includes the “more polar” systems, including LiH, HF, BeF, BeO, NaCl, and LiF, etc. These are all examples of diatomics that actually aggregate to form ionic solids or H-bonded networks in the condensed phase. Nuclear-resisted bonds, in contrast, are found, in general in “less polar” molecules. We note that part of the exceptions to this rule include all of those systems with “reversed polarity” (contrasting their dipole moments with what might have been expected from classical Pauling electronegativity arguments), BF, CO, NO, and CF. We will soon see that there is something special about one of the other exceptions with a relatively large dipole moment, BO; it inhabits a small intermediate region where both $\Delta\bar{\chi}$ and $n^{-1}\Delta(V_{\text{NN}} + \omega)$ are negative.

There is a method to our madness in including $\text{H} + \text{e} \rightarrow \text{H}^-$ in this table; this will be explained in time.

■ TRYING TO UNDERSTAND POLARITY

Is it surprising that both bond types, nuclear-resisted and multielectron-favored, arise in polar molecules, and that the more polar ones are multielectron-favored? Let us try to get a feeling for what happens in polar bond formation, by looking at two heteronuclear molecules, LiF and CO, one quite polar, one much less so. Consider forming the two from neutral atoms, but now in stages, starting with initial electron transfer between atoms, followed by recombination, as in eq 8:



As far as the energy changes go, we know them, intuitively. Bond formation from the neutral is exothermic, as is electron attachment. It takes energy to ionize any atom, and it always takes more energy than one obtains by electron attachment to its bonding partner. So in diatomic bond formation, the second step, recombination of the ions, is highly exothermic, enough to overcome the difference between the ionization potential and the electron affinity of the first steps.

We summarize the changes in $\Delta\bar{\chi}$ and $\Delta\omega/n$ for the elementary steps in the first stage of the reaction taken apart in this way, in Table 4. $\Delta\bar{\chi}$ is always positive for electron attachment, and negative for ionization. Just as one would expect, orbital energies go up in the former, down in the latter.

Table 4. Typical Values for the Hypothetical First Step in Scheme 1^a

	$\Delta E/n^b$	$\Delta\bar{\chi}^c$	$\Delta\omega/n$	classification
$\text{C} \rightarrow \text{C}^+ + \text{e}^-$	+1.88	-9.56	+11.44	m.e.-resisted
$\text{C} + \text{e}^- \rightarrow \text{C}^{-a}$	-0.17	+7.36	-7.53	m.e.-favored
$\text{O} \rightarrow \text{O}^+ + \text{e}^-$	+1.70	-12.63	+14.33	m.e.-resisted
$\text{O} + \text{e}^- \rightarrow \text{O}^{-a}$	-0.15	+10.52	-10.67	m.e.-favored
$\text{Li} \rightarrow \text{Li}^+ + \text{e}^-$	+1.80	-4.09	+5.89	m.e.-resisted
$\text{Li} + \text{e}^- \rightarrow \text{Li}^{-a}$	-0.22	+3.42	-3.58	m.e.-favored
$\text{F} \rightarrow \text{F}^+ + \text{e}^-$	+1.94	-14.41	+16.35	m.e.-resisted
$\text{F} + \text{e}^- \rightarrow \text{F}^{-a}$	-0.34	+12.02	-12.36	m.e.-favored
$\text{Li} + \text{F} \rightarrow \text{Li}^+ + \text{F}^-$	+1.99	+8.99	-8.83	m.e.-favored

^aAs a general rule, electron attachment reactions are always multielectron-favored. Either of the previously defined¹ classifications “binding” or “multielectron” is strictly applicable here, because $\Delta V_{\text{NN}}/n = 0$. All energies are in eV e^{-1} . “Multielectron” is here abbreviated by m.e. ^bExperimental data from NIST Chemistry WebBook, except electron affinities, which are calculated at the G4 level. ^cFrom LC-BLYP/aug-cc-pVQZ calculations.

$\Delta\omega/n$ behaves in the opposite way; it is negative for electron attachment, positive for ionization. $\Delta V_{\text{NN}}/n = 0$ in any ionization, so $\Delta(V_{\text{NN}} + \omega)/n = \Delta\omega/n$. The changes in multielectron interactions are greater in magnitude (if they were not there would never be a positive electron affinity) than $\Delta\bar{\chi}$. This is the reason why all of these electron attachment/detachment steps are multielectron-favored/-resisted. A large $\Delta\omega/n$ term is intimately associated with electron transfer, which is why it will soon figure importantly in a measure of bond character. Clearly the formation of ions, exothermic or endothermic, is multielectron-resisted or -favored.

Note that in Table 4 we also have included the electron attachments/detachments “the wrong way around”, that is, $\text{Li} \rightarrow \text{Li}^-$ and $\text{F} \rightarrow \text{F}^+$. This is because we expect to learn something from putting the molecule together in an unconventional way.

Continuing with the second step in eq 8 when A^+ and B^- are brought together, $\Delta V_{\text{NN}}/n$ is turned on, so to speak. This term is always large and positive, resisting bonding. Table 5 shows the energy components for bond formation in this ionic recombination step. It includes, for comparison, the partitioning for assembly of the diatomic from neutral atoms (this was already shown in Table 3). In moving between Tables 4 and 5, it is important to recall that the energy components are per electron, that is, 3 electrons for $\text{Li} \rightarrow \text{Li}^+ + \text{e}^-$, 10 electrons for $\text{F} + \text{e}^- \rightarrow \text{F}^-$, and 12 electrons for $\text{Li} + \text{F} \rightarrow \text{LiF}$.

We also feel it necessary to reiterate our convention for classifying reactions as -favored or -resisted in a classification does not imply that the overall reaction is exo- or endothermic. It denotes the single component of the three parts of the energy that goes in a direction opposite to the other two. So exothermic $\text{C} + \text{O} \rightarrow \text{CO}$ is nuclear-resisted (in fact orbitals and multielectron terms overcoming nuclear repulsion), while endothermic $\text{Li} + \text{F} \rightarrow \text{Li}^+ + \text{F}^-$ at infinite separation is multielectron-favored (the destabilizing orbital term overcomes the stabilizing multielectron factor).

The classification of the second stage in eq 8, that is, $\text{A}^+ + \text{B}^- \rightarrow \text{AB}$, will depend greatly on the nature of A and B. Table 5 explains by example; in reactions that begin from an “unfavorable” polarity, such as $\text{Li}^- + \text{F}^+ \rightarrow \text{LiF}$, a large degree of charge transfer should be expected in this last step of bond formation. Just as we noted for electron attachment, this is reflected by the multielectron-favored reaction classification. If instead a polar species, such as LiF, is formed from moieties that are already ionized in the “right” manner, little charge transfer will occur upon bond formation. The ΔV_{NN} term, always positive when atoms come together, then dominates. The net outcome is a situation analogous to the formation of more covalent bonds, a nuclear-resisted process.

Scheme 1. Formation of Any Chemical Bond Dissected into Two Hypothetical Electron Attachment and Detachment Steps, Followed by a Recombination of the Resulting Ions

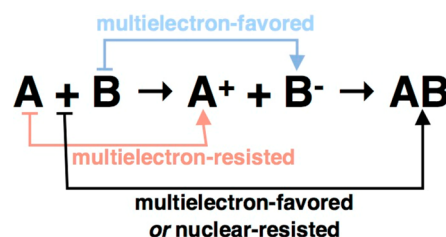


Table 5. Energy Partitioning Components for the Hypothetical Second Step in Scheme 1^a

	$\Delta E/n^b$	$\Delta\bar{\chi}^c$	$\Delta(V_{\text{NN}} + \omega)/n$	$\Delta V_{\text{NN}}/n^b$	$\Delta\omega/n$	classification
$\text{Li}^+ + \text{F}^- \rightarrow \text{LiF}$	-0.67	-4.96	+4.29	+20.72	-16.42	nuclear-resisted
$\text{Li}^- + \text{F}^+ \rightarrow \text{LiF}$	-1.90	+28.4	-30.31	+20.72	-51.03	multielectron-favored
$\text{Li} + \text{F} \rightarrow \text{LiF}$	-0.505	+4.03	-4.54	+20.72	-25.25	multielectron-favored
$\text{C}^+ + \text{O}^- \rightarrow \text{CO}$	-1.52	+4.94	-6.46	+43.76	-50.22	multielectron-favored
$\text{C}^- + \text{O}^+ \rightarrow \text{CO}$	-1.69	+14.40	-16.09	+43.76	-59.85	multielectron-favored
$\text{C} + \text{O} \rightarrow \text{CO}$	-0.806	-2.02	+1.22	+43.76	-42.54	nuclear-resisted

^a“Appropriately” preionized species will not engage in charge transfer upon combination, whereas unfavorably ionized species will. This is reflected by the sign of $\Delta\bar{\chi}$, and by the reaction classification. All energies are in eV e⁻¹. ^bExperimental data from NIST Chemistry WebBook combined with G4 level calculations. ^cFrom LC-BLYP/aug-cc-pVQZ calculations.

If we consider a less polar bond, such as that in CO (as implied by its minute dipole moment), then the creation of the bond from either preionized options will require substantial charge transfer, and both such ionic reactions classify as multielectron favored (Table 5). Scheme 1 summarizes the character of the various stages in this way of looking at the bond-forming reaction. The dissection we made (first electron transfer then recombine ions) was meant to demonstrate the connection between charge transfer and ω . We must stress that in a real bond-formation process all “steps” will, of course, occur simultaneously.

Clearly the multielectron classification is related to charge transfer. We see it in isolated electron transfer, either ionization or attachment. Yet we also see it dominating the energy partitioning in the formation of polar bonds. How can we exploit this connection to gain further insight into chemical bonding?

■ A REASON FOR USING THE COMPOSITE $\Delta(V_{\text{NN}} + \omega)/n$

We postulate that the multielectron-favored bonds, where $\Delta\omega/n$ is the only negative term in the energy expression (eq 2), describe situations where bonds are formed fundamentally due to intramolecular charge transfer. The reasoning is simple; for electron–electron interactions to change, charges must move. We say nothing of the net direction, distribution, or fluctuation in time of this charge, only that a negative $\Delta\omega/n$ -term implies a favorable degree of electron transfer within the molecule upon bond formation.

$\Delta\omega$ is negative in both nuclear-resisted and multielectron-favored bonds. This is because the largest part of $\Delta\omega$ arises as an effective cancellation to ΔV_{NN} , that is, as a simple consequence of electrons in atoms or molecules being brought closer together, not due to subtleties of bonding per se. To quantify how much of $\Delta\omega$ is not a simple consequence of canceling the nuclear–nuclear repulsion, described by a positive ΔV_{NN} , it is necessary to consider the sum $\Delta(V_{\text{NN}} + \omega)/n$, and not just $\Delta\omega$. $\Delta(V_{\text{NN}} + \omega)/n$ describes how well changing nuclear–nuclear repulsions, ΔV_{NN} , are screened by changing multielectron interactions, $\Delta\omega$.

■ CONNECTING COVALENCE TO $\Delta\bar{\chi}$

In the chemical community, a covalent bond is thought of as a bond in which electrons are shared about equally in bond formation. H₂ serves as a paradigm for this kind of bonding, and so does the familiar picture of two orbitals interacting, one going down, one going up in energy. We are well aware of the historical emphasis of the role of the Heitler–London wave function in describing covalent bonding, but wish to focus on energy changes in bond formation. People think of a covalent

bond as one governed by the stabilization of orbitals, and the electrons that occupy them. We have just such a measure of the stabilization of electrons in their average binding energy, $\bar{\chi}$, from theory or experiment.

Because $\Delta\bar{\chi}$ describes the net change in the binding energy of electrons (or the net stabilization of orbitals), the connection between “covalency” and eq 2 becomes clearer; the more $\Delta\bar{\chi}$ contributes to the bond formation, the more covalent is the bond. The other term in the energy expression, $\Delta(V_{\text{NN}} + \omega)/n$, describes the multielectron (or, as we have argued, the charge transfer) character of a bond. As we shall see, large multielectron (i.e., $\Delta(V_{\text{NN}} + \omega)/n$ -dominated) character will be found in what we consider ionic bonds, such as NaCl, and in more “metallogenic” bonds, such as Na₂, as well as in highly correlated bonds, such as F₂.

Let us see how these ideas of $\Delta(V_{\text{NN}} + \omega)/n$ characterizing electron transfer, $\Delta\bar{\chi}$ covalence, can be transformed into a more quantitative measure.

■ SETTING UP CRITERIA FOR BOND CHARACTER

Suppose we use the ratio $\Delta\bar{\chi}/[\Delta E/n]$ to measure how important the $\Delta\bar{\chi}$ -term is in the bond energy, $\Delta E/n$. Similarly, let us take the $[\Delta(V_{\text{NN}} + \omega)/n]/[\Delta E/n]$ ratio, also dimensionless, as an expression of how important the $\Delta(V_{\text{NN}} + \omega)/n$ term is. The difference between the two ratios, here denoted by Q in eq 9, we posit is a measure of how important the first term, which we associate with covalence, is with respect to the second, which relates to intramolecular charge transfer, or multielectron interactions.

$$Q = \frac{\text{“covalency”}}{\Delta\bar{\chi}} - \frac{\text{multielectron-contribution}}{\Delta(V_{\text{NN}} + \omega)/n} = \frac{\Delta E/n}{\Delta\bar{\chi}} - \frac{\Delta E/n}{\Delta(V_{\text{NN}} + \omega)/n} = \frac{\Delta\bar{\chi} - \Delta(V_{\text{NN}} + \omega)/n}{\Delta\bar{\chi} + \Delta(V_{\text{NN}} + \omega)/n} = \frac{K - 1}{K + 1} = \frac{2n\Delta\bar{\chi}}{\Delta E} - 1$$

$$K = \frac{\Delta\bar{\chi}}{\Delta(V_{\text{NN}} + \omega)/n} \quad (9)$$

$$\Delta E/n = \Delta\bar{\chi} + \Delta(V_{\text{NN}} + \omega)/n \quad (2^*)$$

Q , with a little bit of algebra, is the difference divided by the sum of the two terms $\Delta\bar{\chi}$ and $\Delta(V_{\text{NN}} + \omega)/n$. Q can also be expressed as a function of the $\Delta\bar{\chi}/[\Delta(V_{\text{NN}} + \omega)/n]$ ratio K . From the last of the several expressions for Q , we can see that to determine Q one only needs ΔE and $\Delta\bar{\chi}$. Not having to evaluate ΔV_{NN} explicitly is advantageous, as this term blows up in a large system, or in a periodic calculation.

Q is uniquely defined, but arbitrary. There are alternative measures of covalence that can be constructed using the different terms of eq 2. Whereas Q is unbound, such indices could, for instance, be constructed to range between 0–100%. Aside from serving the purpose of connecting the time-honored and intuitively engrained concept of bond covalency as a fraction or percentage, downsides emerge for such scales. This is explored in the Supporting Information.

■ GETTING A FEELING FOR Q

Whereas we recognize that the nature of chemical bonding in homonuclear diatomics can be different (contrast Li_2 , H_2 , F_2), we might nevertheless imagine them all as inherently “covalent”. As Figure 2 shows, things are not so simple.

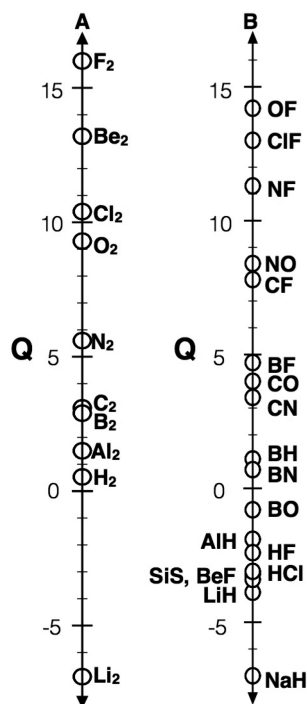


Figure 2. Selected diatomic bonds within the range $-7 < Q < 16$. (A) Homonuclear diatomic bonds, and (B) heteronuclear diatomic bonds.

Homonuclear diatomics exhibit a range of Q between -10 and $+16$, due to great differences in the nature of these bonds. We omit here many weak bonds and weak attractive dispersion force minima; the nature of these “enlarges” the Q space, and they will be discussed separately. Figure 2 also shows heteronuclear diatomic bonds, illustrating that these fill up a space in Q similar to that of the homonuclear ones. However, one notices immediately that the most polar heteronuclear bonds (as measured, for instance, by any classical electro-negativity scale or by dipole moment) have negative Q . These are the multielectron-favored bonds, with a large negative $\Delta(V_{\text{NN}} + \omega)/n$ dominating $\Delta\bar{\chi}$.

How can we interpret this spread in Q ? Clearly Q leads us to a differentiation, an important one, of bonds we normally (and intrinsically) consider as covalent.

For $Q = 1$, $\Delta E = \Delta\bar{\chi}$ (eq 9), that is, $\Delta(V_{\text{NN}} + \omega)/n$, electron transfer, is entirely unimportant. In contrast, where $Q = -1$, the bond is completely dominated by the $\Delta(V_{\text{NN}} + \omega)/n$ -term. Here, various multielectron interactions govern the bond. We see from Figure 2 that only very few bonds fall into the range

$-1 < Q < 1$, specifically only BN ($Q = 0.7$), H_2 ($Q = 0.5$), and BO ($Q = -0.8$). H_2 is closest to the special point of $Q = 0$, where $\Delta\bar{\chi} = \Delta(V_{\text{NN}} + \omega)/n$. It can be interpreted as a crossover between “covalent” and “ionic”.

Table 6 and Scheme 2 summarize a set of different regimes in Q , and their interpretation, which will be further justified below.

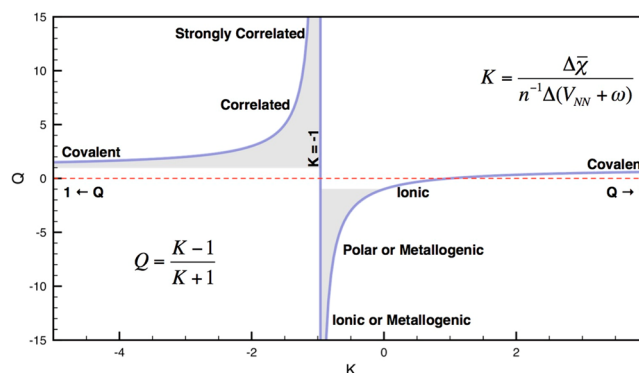
Table 6. Criteria for Bond Character and Interpretation^a

$\Delta\bar{\chi}$	$\Delta(V_{\text{NN}} + \omega)/n$	Q	interpretation
–	+	$Q > 1$	correlated, electrostatic, dispersion
–	0	$Q = 1$	covalent
– ^b	– ^b	$Q = 0$	mixed
0	–	$Q = -1$	ionic
+	–	$Q < -1$	polar, ionic, metallogenic

^aThroughout bond formation is exothermic; that is, ΔE is negative.

^b $\Delta\bar{\chi} = \Delta(V_{\text{NN}} + \omega)/n$.

Scheme 2. Relationship between Q and K Shown Together with the Type of Bonds Found in Different Regions^a



^aRegions where $Q > 1$ and $Q < -1$ are shaded.

Situations where $1 < Q < -1$ describe in different ways how multielectron interactions become more important, acting either with or against the bond’s formation.

How can Q be greater than 1 or less than -1 ? From eq 9, we see that this happens for negative K ; that is, $\Delta\bar{\chi}$ and $\Delta(V_{\text{NN}} + \omega)/n$ must be of opposite sign. When the terms are of opposite signs, their relative magnitude determines Q : If $|\Delta\bar{\chi}| > |\Delta(V_{\text{NN}} + \omega)/n|$, then Q will be bigger than 1, while if $|\Delta\bar{\chi}| < |\Delta(V_{\text{NN}} + \omega)/n|$, Q will be less than -1 . The regimes where Q is more than 1, and less than -1 , happen only near $K = -1$ (Scheme 2). $Q > 1$ for all K more negative than -1 , and $Q < -1$ for the restricted region $-1 < K < 0$. Note that situations with $Q =$ exactly -1 , 0 , $+1$ by definition involve rare circumstances of either $\Delta\bar{\chi}$ or $\Delta(V_{\text{NN}} + \omega)/n$ equal to zero, or equal to each other (Table 6).

If we have bond formation-disfavoring multielectron contributions, as described by a positive $\Delta(V_{\text{NN}} + \omega)/n$ -term, we move toward more positive Q (defining eq 9; note ΔE is negative). As we suspect from looking in detail at Figure 2, this situation appears for bonds where “electron correlation” plays an increasing role, such as in O_2 and F_2 . We will soon make more precise the correlation attribute. In the other case, where $Q < -1$, the $\Delta(V_{\text{NN}} + \omega)/n$ -term is instead negative (and larger in magnitude than $\Delta E/n$). This we have already seen is indicative of polar and ionic bonds, and for homonuclear bonds a more special situation exemplified by Li_2 , and other metallogenic diatomics. What we mean by the metallogenic

neologism (used also in Table 6 and Scheme 2), to anticipate a more detailed discussion, is elements that have low ionization potentials, and that upon building up of a cluster, $M \rightarrow M_2 \rightarrow M_3 \rightarrow M \rightarrow \dots M_n$, undergo an insulator to metal transition.

Q by itself is not enough to clearly differentiate bond types. Another dimension is hinted at, if informative partitioning of the great variety of bond types we know is to be attained. In the spirit of remaining with experimentally measured variables, we next consider the total energy change in a reaction.

■ Q AND ΔE

We plot in Figure 3 Q for 50 diatomic bonds (including H^-) against the most important measure we have of a chemical

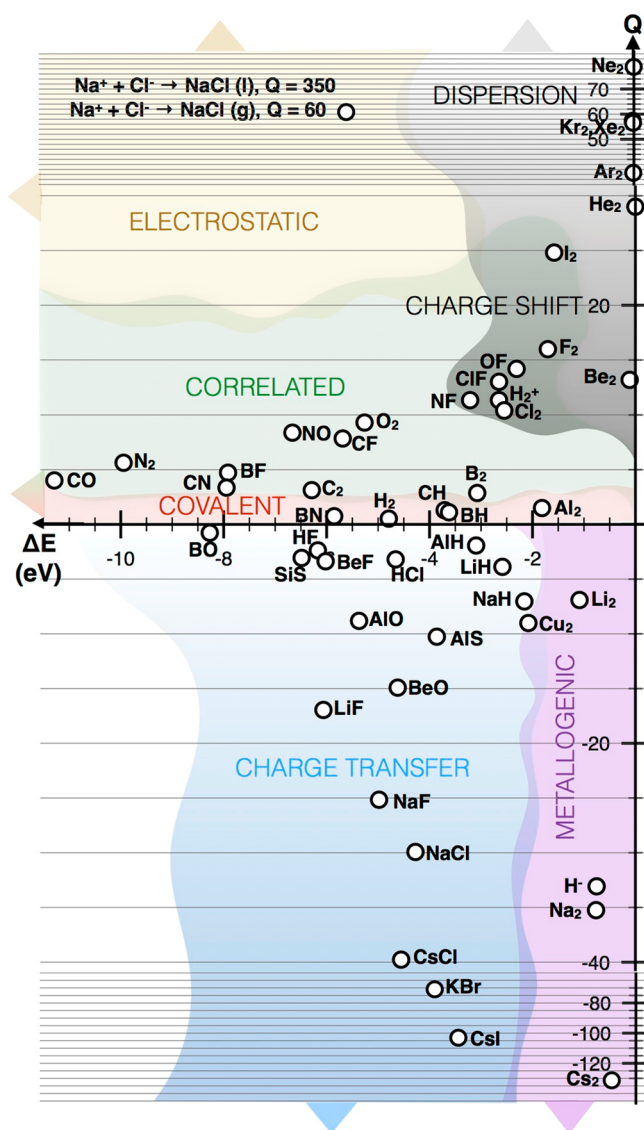


Figure 3. The Q -scale plotted against the bond dissociation energy ΔE in a range of diatomics reveals familiar groups of chemical interactions.

bond, the dissociation energy, ΔE . Now a better separation is achieved of the variety of bonds one finds in chemistry. We discuss the different regions of this diagram in detail.

■ “COVALENT” BONDS

Typical strong bonds are associated with covalence, positive Q , but not necessarily that close to $Q = 1$. Nor should we expect

that $Q = 1$ is a singular point with $\Delta(V_{NN} + \omega)/n = 0$. The bond closest to $Q = 1$ is actually a heteronuclear one, BH ($Q = 1.1$). In this simple case, the near unity Q can be understood from the bonding σ_u orbital, which is constructed by a near perfect overlap of the $1s^1$ of H with one lobe of the $2p^1$ on B. The good overlap, along with a small number of interacting valence electrons, a feature that minimizes the importance of same-spin repulsion, merits only minor deformation of formal atomic orbitals (which would translate into intramolecular charge transfer and thus a $\Delta(V_{NN} + \omega)/n$). Similar arguments of good overlap and minor exchange energy contributions can be made to explain the predicted covalency (Q near 1) of bonds in species such as CH, BN, H_2 , and Al_2

■ POLAR AND IONIC BONDS

Remaining with strong bonds, a high magnitude of ΔE , we find highly polar and ionic diatomics in the bottom center domain in Figure 3, where they take on negative values of Q . Examples include HF ($Q = -2.4$), NaH ($Q = -7.0$), LiF ($Q = -17.0$), NaCl ($Q = -29.9$), CsCl ($Q = -39.8$), KBr ($Q = -70.9$), and CsI ($Q = -103.0$). In strongly ionic bonds, the intramolecular electron transfer character captured by Q can be attributed to single-electron charge transfer. We will return to the specific example of NaCl below.

■ “CORRELATED” BONDS

As we go to positive values in Q , while remaining in the relatively high ΔE region, we encounter species characterized by increasing degrees of “electron correlation”. What do we mean by “correlation”? Within quantum chemistry, correlation energy has a specific meaning. It is usually defined as the difference between the exact energy and that obtained from a single-reference Hartree–Fock calculation extrapolated to the basis set limit. Such a calculation treats an important part of all multielectron interactions, the same-spin (i.e., exchange or Pauli) repulsion. Higher order electron interaction effects are left untreated. The definition of correlation energy is very theory-centric; there is no clear experimental measure of the quantity.

To make matters worse, correlation energy is not the same as electron correlation, which relates to the physical picture of correlated movement of electrons due to all of their different interactions. One way out of a nightmare of arguably confusingly similar definitions is our usage of the word “multielectron”, which includes all types of interactions between electrons (here quantified by ω).

In what follows, “correlation energy” refers to the missing Hartree–Fock energy. This is distinct from “electron correlation”, “correlation”, or “correlated bonds”, which all refer to the physical picture of electrons moving in correlated manners due to any number of multielectron interactions.

As we have learned from the special case of F_2 , homonuclearity or a good Lewis structure is not a guarantee that a simple quantum mechanical calculation (i.e., Hartree–Fock) will give bonding. One needs to account for correlation explicitly and carefully. Even bonds thought to be “normal”, such as the strong triple bond of N_2 , are substantially “correlated”; 50% of the bond energy of N_2 is due to correlation effects beyond the Hartree–Fock level.⁸⁷

Figure 4 plots the missing correlation energy (measured as % of the bond energy) versus Q for selected diatomics. We will discuss several specific trends in detail below; what is clear from

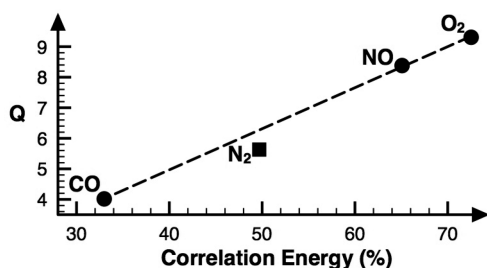


Figure 4. Q for selected nuclear-resisted diatomic oxides and molecular nitrogen plotted versus the correlation energy of the bonds. The correlation energy here is given as the percentage of the total bond energy that comes from moving beyond the Hartree–Fock limit.

Figure 4 is that large Q bonds are strongly correlated. Why should this be so? It is because in our analysis ω summarizes all multielectron interactions. These include many useful and familiar divisions, such as exchange, static, and dynamic correlation, as well as pure electrostatics. For this reason, we can expect a linear relationship like that shown in Figure 4 when the reasons behind a trend in chemical bonding lie beyond a Hartree–Fock description.

Several examples of “correlated” diatomics appear in Figure 3, for example, C_2 ($Q = 3.1$) and O_2 ($Q = 9.3$). F_2 , the archetypical charge-shift bond,⁸³ attains the high value of $Q = 16.0$. We do not include it in Figure 4; if we did, its correlation energy would exceed 100% of the bond energy; that is, there is no bond in F_2 at the Hartree–Fock limit.^{88–90}

In Figure 3, the bond in F_2 borders with another region inhabited by diatomic aggregates characterized by fluctuating interactions, the much weaker dispersion interactions.

■ WEAK DIATOMIC BONDS OR DISPERSION FORCE ASSOCIATIONS

We note first that there are larger uncertainties in the Q values of dispersion-bound associations because of the way Q is defined, with ΔE in the denominator. At the top of the diagram, we have attractive dispersion interactions as in the dimers He_2 ($Q \approx 29$), Ar_2 ($Q \approx 37$), Kr_2 ($Q \approx 57$), Xe_2 ($Q \approx 57$), and Ne_2 ($Q \approx 79$). The Q values of these extremely weakly bound (μeV) interactions are especially uncertain due to technical difficulties in accurately calculating $\Delta\bar{\chi}$. Even though Q values for the noble gas dimers vary with basis set, Q is consistently found to be high and positive (>20). Dispersion interactions arise due to fluctuations in the electron density, and represent one form of intramolecular (over time, isotropic) charge transfer.

■ METALLOGENIC BONDS

More interesting are the negative Q , low ΔE , species Li_2 ($Q = -6.9$), Na_2 ($Q = -35.2$), Cs_2 ($Q = -131.2$), and H^- ($Q = -33.1$). These have weakly bound outmost electrons, and that is a feature we also associate with metallic character. Also, as these aggregate into larger clusters (not yet studied by us), the clusters quickly become metallic. We expect diatomics of the transition series to fall into this region as well. Indeed, Cu_2 ($Q = -9.0$), one of few transition metal dimers described reasonably accurately with DFT methods,⁹¹ does tell the same story. We note that some diatomics, AlH , LiH , NaH , are close to the metallogenic region. Indeed there are calculations that suggest that under pressure LiH undergoes an insulator-to-metal

transition.⁹² The relationship between Q , low ΔE , and pressure-induced metallicity remains to be explored.

■ ELECTROSTATIC INTERACTIONS

Finally, purely electrostatic interactions, that is, strong interactions formed without preceding intramolecular electron transfer (like those we discussed earlier), attain very large and positive values of Q and reside in the upper left corner of Figure 3. One telling example is found in the $NaCl$ diatomic.

The diatomic $NaCl$, of course unstable to assembly into an $NaCl$ crystal, is nevertheless relatively strongly bound, and has an internuclear separation smaller than that in the crystal. The process of $NaCl$ formation has a low Q -value of -29.9 . As shown earlier in the context of Table 3, this is a multielectron favored process, $\Delta\bar{\chi} = +2.2 eV e^{-1}$, and we therefore expect it to be governed by some form of intramolecular electron transfer. The low Q -value and the classification as multielectron-favored support a well-known interpretation of the $Na + Cl$ potential energy surface, starting out at long separations with a covalent MO formulation, followed by a quick crossover to a mainly ionic potential energy curve.^{93,94} One then has single-electron charge transfer, leaving us with the Na^+Cl^- description.

What if we instead consider the bonding event in water solution, where one reasonable pathway to $NaCl$ is the union of solvated Na^+ and Cl^- ions? We can approximate this process computationally simplistically, by treating the effect of a water environment by an implicit solvation model, described in the Methodology. When we do so, we find that this bond formation, in contrast to the gas-phase process, is nuclear-resisted ($\Delta\bar{\chi} = -5.6 eV e^{-1}$). Of course, the nuclear-resisted classification implies that intramolecular electron transfer should not be governing. This is expected because in this situation the components Na^+ and Cl^- are already “pre-polarized” and no electron transfer is required to form the preferred state. To reflect this change in reference from the gas phase into the liquid phase, the Q -value rises significantly to +350!

If we consider the union of Na^+ and Cl^- in the gas phase (i.e., without a stabilizing chemical environment), then the Q value is lowered, but remains high, at +60. Both of these high values of Q are far greater than what is reasonable for covalent bonds. The strength of the interaction (counted per electron) also rules out dispersion interactions. This leaves us with Coulomb interactions between oppositely charged ions, interactions that also are a form of multielectron interactions. This exemplifies how we can arrive at the same Na^+Cl^- description, but from different starting points, and in different chemical environments. In this analysis, the nature of chemical bonds is not static. Instead their nature is a reflection of the process that formed them.

■ THE CONNECTION BETWEEN Q AND ELECTRON CORRELATION

We have seen how Q expresses differences in chemical bonding, and we have discussed how different regions in Q versus ΔE coincide with familiar bonding types. What more does this analysis have to offer for the rationalization and conceptualizing of chemical bonding? Capturing the correlation energy is one of the central challenges in quantum chemistry. As was already mentioned, correlation energy is defined as the energy difference between the exact total energy and that obtained following an infinite basis set Hartree–Fock calculation. A large

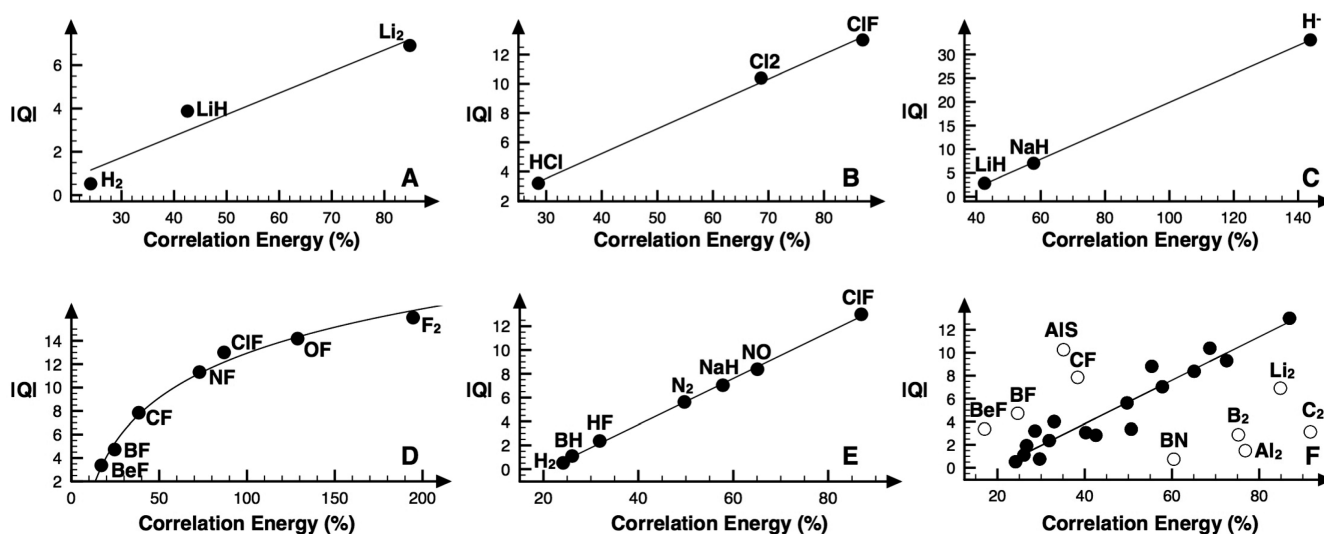


Figure 5. Q 's relation to electron correlation for several series of diatomics. The absolute of Q was used in these plots to allow inclusion and show linear correlation with select multielectron-favored bonds. The correlation energy here is given as the percentage of the total bond energy that comes from moving beyond the Hartree–Fock limit. (A) The $H_2 \rightarrow LiH \rightarrow Li_2$ progression. (B) The $HCl \rightarrow Cl_2 \rightarrow ClF$ progression. (C) Alkali metal hydrides \rightarrow free hydride. (D) Investigated fluorides show an exponential relationship (LiF and NaF excluded). (E) Various diatomics exhibiting especially clear correlation between Q and correlation energy. (F) All investigated diatomics excluding species with $|Q| > 13.0$ and all weak dispersion interactions.

positive Q value implies the presence of multielectron effects. But, as we now show, only a part of all multielectron effects can be related to the missing correlation energy.

Let us begin with the isoelectronic series, N_2 , CO, BF. Carbon monoxide has the strongest known chemical bond (11.3 eV), which includes 33% correlation energy. CO is isoelectronic with N_2 (50% correlation energy). How does one make sense of the differences and similarities between these formally isoelectronic species? Because we in this instance know that the bonds have quite sizable correlation energy contributions (which is one subset of the multielectron contributions captured by ω), we should expect Q values larger than 1. Indeed, $Q_{N_2} = 5.6$ and $Q_{CO} = 4.2$. In this case, the difference in Q between the two compounds can be largely attributed to a difference in the electron correlation energy. The reason is as follows: the ratio of $Q_{N_2}/Q_{CO} = 0.65$ is near identical to the quotient of the percentage of electron correlation contributions to the bonds, $E_{\%corr,N_2}/E_{\%corr,CO} = 0.66$, calculated by comparing Hartree–Fock energies with experiment (Figure 4 and Supporting Information). O_2 and NO are two other near neighbors in the same domain in Figure 3 ($Q_{O_2} = 9.3$ and $Q_{NO} = 8.4$). The ratio of $Q_{O_2}/Q_{NO} = 1.11$ is again nearly identical to the corresponding correlation energy percentage ratio, $E_{\%corr,O_2}/E_{\%corr,NO} = 1.11$.

BF has a Q value of 4.7, which is intermediate between those of CO and N_2 , with which BF is formally isoelectronic. However, BF's inherent correlation energy is 25%, and in this case there is no good agreement between the Q and E_{corr} -ratios comparing $BF \leftrightarrow CO$ and $BF \leftrightarrow N_2$. Why not? This is because the physical difference between these bonds is not only due to correlation energy. Instead the difference is already apparent from effects treated well by a simple Hartree–Fock wave function (such as exchange repulsion). To put it differently, multielectron interactions de facto increase as we proceed in the order $CO \rightarrow BF \rightarrow N_2$, but the nature of the interactions responsible for this trend is not treated consistently by a one-particle mean-field theory such as Hartree–Fock (Figure 4).

Figure 5 illustrates numerous tantalizing correlations between Q and the correlation energy of various bonds, to add to the one already shown in Figure 4. To include multielectron-favored bonds (which have negative Q), we have plotted the absolute value of Q versus correlation energy in Figure 5. As discussed above, both negative and positive Q values signify the presence of multielectron-interactions, albeit with different physical interpretations. In the cases where collections of bonds fall on the same line in a Q versus correlation energy plot, such as $H_2 \rightarrow LiH \rightarrow Li_2$, or $CO \rightarrow N_2 \rightarrow NO \rightarrow O_2$, the inherent differences between these bonds can be directly attributed to differences in correlation energy (i.e., by effects beyond the mean field Hartree–Fock description). In contrast, nonlinear relationships between bonds imply that effects correctly treated by Hartree–Fock, such as exchange interactions and Coulombic interactions, better explain the nature of the differences.

Figure 5F shows the correlation of the absolute value of Q with % correlation energy for all diatomics investigated whose $|Q| < 13$. Note what seems to be the approximately linear behavior, but along several straight lines. We continue to explore this tantalizing relationship.

The Q –correlation connection illustrates, and reminds us, that differences in the nature of certain bonds cannot always be found within an independent particle model. Sometimes energy trends, or differences between bonds, arise due to subtle differences in the correlated movement of electrons. Rationalizing the collective will of electrons is and will likely remain a challenge. We suggest that ω is a useful expression of multielectron interactions, all of them, and that Q , by extension, is a window into the nature of the chemical bond.

CONCLUSIONS

This work begins by recapitulating the basics of a different kind of energy partitioning scheme. Its basic tenet is that the energy of any interaction, irrespective of its magnitude, is always described by $\Delta E/n = \Delta\bar{\chi} + \Delta(V_{NN} + \omega)/n$ (eq 2). $\Delta\bar{\chi}$ describes

the average change of electron binding energies upon bond formation, in molecular orbital terminology, the stabilization or destabilization of the average orbital. $\Delta(V_{\text{NN}} + \omega)/n$ describes how well changing nuclear–nuclear repulsions, ΔV_{NN} , are screened by changing multielectron interactions, $\Delta\omega$. $\Delta\omega$ can, in principle, be dissected into many useful and familiar terms, including, for instance, static and dynamic correlation, electrostatics, as well as dispersion interactions (a multielectron phenomenon). Yet we follow a different road, keeping ω undivided, and concentrating on obtaining it from experimental observables or theory.

Two paradigms of chemical bond formation arise from this analysis, and we label them nuclear-resisted and multielectron-favored, respectively. In essence, what these two labels distinguish is whether the $\Delta\bar{\chi}$ -term is acting with or against the change in total energy upon bond formation. In the latter case, the formation of a bond or electron attachment in an exoergic reaction is made possible by the introduction of multielectron interactions. Without the latter, positive electron affinities would not exist. Multielectron interactions come to the fore in any process that involves substantial electron shifts to, from, or within a molecule. For heteronuclear diatomics, the bond type, multielectron-favored or nuclear-resisted, groups the bonds into more or less polar, respectively, categories.

Our exploration of bonding leads us to a chemical interaction descriptor called Q . To obtain Q for any given bond (or interaction), we need to experimentally estimate, or quantum mechanically calculate, two quantities, the bond dissociation energy, ΔE , and $\Delta\bar{\chi}$. With these two pieces of information in hand, we can use eq 2 to calculate $\Delta(V_{\text{NN}} + \omega)/n$, which together with $\Delta\bar{\chi}$ provides Q via eq 9.

If we plot Q versus the bond energy, intuitively familiar bonding domains appear (Figure 3). There are no sharp boundaries between these domains, yet we see groups of bonds we associate with being covalent, covalent but more correlated, polar and increasingly ionic, electrostatic, charge-shift bonds, and dispersion interactions. Diatomics that if extended to higher clusters would metallize are also separated. The potential utility of this measure in predicting chemical and physical properties of larger materials by the analysis of smaller subunits exists.

Because ω includes all multielectron interactions, Q sometimes shows striking relationships with the correlation energy contribution to bond energies.

This work has focused on simple diatomics. It is possible to perform our energy partitioning analysis, and consider variations in Q , for much more complex reaction mechanisms, or physical processes, as future work will show.

METHODOLOGY

All experimental data are taken from the *National Institute of Standards and Technology (NIST) WebBook*, unless otherwise specified. All energies are given in electronvolt (eV), or electronvolt per electron (eV e^{-1}). One $\text{eV} = 96.4853 \text{ kJ/mol} = 23.0605 \text{ kcal/mol}$. To approximate the change in energy, ΔE , from experimental heats of formation or reaction, $\Delta H_{\text{f/r}}^0$, and vibrational spectroscopy, the experimental harmonic zero-point energy E_{ZPE} was subtracted, that is, $\Delta E \approx \Delta H^0 - E_{\text{ZPE}}$, where $E_{\text{ZPE}} \approx 1/2h\sum\nu_i$, and where ν_i are the i th fundamental frequencies of the molecule. Experimental structures were used throughout. Dimers of the noble gas elements were calculated using experimental potential well depths and geometries.⁹⁵ The heat of formation for gaseous CsI was taken from ref 96.

With the exception of experimental values for H^- and H_2 , all estimations for $\Delta\bar{\chi}$ were obtained using the range-separated LC-BLYP

density functional. All such calculations used the aug-cc-pVQZ basis set.^{97,98} The exceptions are calculations of $\Delta\bar{\chi}$ for the noble gas dimers, which were done using a Douglas–Kroll–Hess second-order scalar relativistic Hamiltonian^{99–103} and the QZP-DKH basis set.^{104,105} All-electron relativistic calculations on I_2 and CsI were done using the very large uncontracted ANO-RCC basis set. It should be stressed that the choice of functional does not affect the general conclusions reached in this work, nor does it appear to significantly affect $\Delta\bar{\chi}$ values. From a practical standpoint, and contrary to the absolute values of $\bar{\chi}$, estimations of $\Delta\bar{\chi}$, even with small basis sets, are more reliable due to error cancellations. The latter is true irrespective of $\bar{\chi}$ estimated theoretically, or measured experimentally. Caution should be taken when not considering all electrons explicitly. All levels shift slightly upon reaction, even those close to the core. This becomes a concern when treating especially heavy elements using pseudo potentials, which effectively removes the majority of the electrons. A typical pseudopotential-based ($5s^25p^66s^1$) basis set for Cs, for example, only includes 9 out of 55 electrons, or ca. 18% of the total. This is not sufficient to estimate $\Delta\bar{\chi}$ reliably. Estimates to the solvation of Na^+ , Cl^- , and NaCl in water were done by combining LC-BLYP/aug-cc-pVQZ level calculations with the implicit polarizable-continuum SMD method.¹⁰⁶

A python script for reading energies and structures and performing the $\bar{\chi}$ -analysis on molecules and atoms is provided in the Supporting Information of our previous paper.¹ It relies on cclib,¹⁰⁷ which can interpret output from numerous popular quantum chemistry programs.

ASSOCIATED CONTENT

Supporting Information

The Supporting Information is available free of charge on the ACS Publications website at DOI: 10.1021/jacs.5b12434.

Various bond characteristics and data for all investigated diatomics; tests of calculating $\Delta\bar{\chi}$ reliably using different methods; and comments on the possibility of expressing covalence within 0–100% (PDF)

AUTHOR INFORMATION

Corresponding Author

*martinr@kth.se

Notes

The authors declare no competing financial interest.

ACKNOWLEDGMENTS

Our research was supported by the Energy Frontier Research in Extreme Environments (EFREE) Center, an Energy Frontier Research Center funded by the U.S. Department of Energy, Office of Science, under Award number DE-SC0001057. National Science Foundation (NSF) funding through Research Grant CHE 13-05872 is also gratefully acknowledged. Toby Zeng and Peng Xu are acknowledged for valuable discussions.

REFERENCES

- (1) Rahm, M.; Hoffmann, R. *J. Am. Chem. Soc.* **2015**, *137*, 10282–10291.
- (2) Allen, L. C. *J. Am. Chem. Soc.* **1989**, *111*, 9003–9014.
- (3) Allen, L. C. *J. Am. Chem. Soc.* **1992**, *114*, 1510–1511.
- (4) Allen, L. C. *Int. J. Quantum Chem.* **1994**, *49*, 253–277.
- (5) Mann, J. B.; Meek, T. L.; Allen, L. C. *J. Am. Chem. Soc.* **2000**, *122*, 2780–2783.
- (6) Deleuze, M. S.; Cederbaum, L. S. *Adv. Quantum Chem.* **1999**, *35*, 77–94.
- (7) Cederbaum, L. S.; Domcke, W.; Schirmer, J.; Von Niessen, W. *Adv. Chem. Phys.* **1986**, *65*, 115–159.

- (8) Cederbaum, L. S.; Domcke, W.; Schirmer, J.; Von Niessen, W.; Diercksen, G. H. F.; Kraemer, W. P. *J. Chem. Phys.* **1978**, *69*, 1591–1603.
- (9) Pettifor, D. *Bonding and Structure of Molecules and Solids*; Oxford University Press: New York, 1995.
- (10) Burdett, J. K. *Struct. Bonding (Berlin)* **1987**, *65*, 29–90.
- (11) Burdett, J. K.; Lee, S. *J. Am. Chem. Soc.* **1985**, *107*, 3050–3063.
- (12) Burdett, J. K.; Lee, S. *J. Am. Chem. Soc.* **1985**, *107*, 3063–3082.
- (13) Politzer, P.; Murray, J. S.; Bulat, F. A. *J. Mol. Model.* **2010**, *16*, 1731–1742.
- (14) Murray, J. S.; Shields, Z. P.-I.; Lane, P.; Macaveiu, L.; Bulat, F. A. *J. Mol. Model.* **2013**, *19*, 2825–2833.
- (15) Toro-Labbe, A.; Jaque, P.; Murray, J. S.; Politzer, P. *Chem. Phys. Lett.* **2005**, *407*, 143–146.
- (16) Politzer, P.; Peralta-Inga, S.; Zenaida; Bulat, F. A.; Murray, J. S. *J. Chem. Theory Comput.* **2011**, *7*, 377–384.
- (17) Jin, P.; Murray, J. S.; Politzer, P. *Int. J. Quantum Chem.* **2004**, *96*, 394–401.
- (18) Politzer, P.; Murray, J. S.; Grice, M. E.; Brinck, T.; Ranganathan, S. *J. Chem. Phys.* **1991**, *95*, 6699–6704.
- (19) Pauling, L. *J. Am. Chem. Soc.* **1932**, *54*, 3570–3582.
- (20) Mulliken, R. S. *J. Chem. Phys.* **1934**, *2*, 782–793.
- (21) Gordy, W. *Phys. Rev.* **1946**, *69*, 604–607.
- (22) Walsh, A. D. *Proc. R. Soc. London, Ser. A* **1951**, *207*, 13–30.
- (23) Sanderson, R. T. *Science (Washington, DC, U. S.)* **1951**, *114*, 670–672.
- (24) Allred, A. L.; Rochow, E. G. *J. Inorg. Nucl. Chem.* **1958**, *5*, 264–268.
- (25) Iczkowski, R. P.; Margrave, J. L. *J. Am. Chem. Soc.* **1961**, *83*, 3547–3551.
- (26) Parr, R. G.; Donnelly, R. A.; Levy, M.; Palke, W. E. *J. Chem. Phys.* **1978**, *68*, 3801–3807.
- (27) Sanderson, R. T. *J. Am. Chem. Soc.* **1983**, *105*, 2259–2261.
- (28) Pearson, R. G. *J. Am. Chem. Soc.* **1985**, *107*, 6801–6806.
- (29) Reed, J. L. *J. Phys. Chem.* **1991**, *95*, 6866–6870.
- (30) Ghosh, D. C. *J. Theor. Comput. Chem.* **2005**, *4*, 21–33.
- (31) Putz, M. V. *Int. J. Quantum Chem.* **2006**, *106*, 361–389.
- (32) Ferro-Costas, D.; Perez-Juste, I.; Mosquera, R. A. *J. Comput. Chem.* **2014**, *35*, 978–985.
- (33) Boyd, R. J.; Edgecombe, K. E. *J. Am. Chem. Soc.* **1988**, *110*, 4182–4186.
- (34) Boyd, R. J.; Boyd, S. L. *J. Am. Chem. Soc.* **1992**, *114*, 1652–1655.
- (35) Frenking, G.; Froehlich, N. *Chem. Rev. (Washington, DC, U. S.)* **2000**, *100*, 717–774.
- (36) Matito, E.; Sola, M. *Coord. Chem. Rev.* **2009**, *253*, 647–665.
- (37) Kitaura, K.; Morokuma, K. *Int. J. Quantum Chem.* **1976**, *10*, 325–340.
- (38) Ziegler, T.; Rauk, A. *Inorg. Chem.* **1979**, *18*, 1558–1565.
- (39) Bagus, P. S.; Hermann, K.; Bauschlicher, C. W., Jr. *J. Chem. Phys.* **1984**, *80*, 4378–4386.
- (40) Bagus, P. S.; Hermann, K.; Bauschlicher, C. W., Jr. *J. Chem. Phys.* **1984**, *81*, 1966–1974.
- (41) Stevens, W. J.; Fink, W. H. *Chem. Phys. Lett.* **1987**, *139*, 15–22.
- (42) Glendening, E. D.; Streitwieser, A. *J. Chem. Phys.* **1994**, *100*, 2900–2909.
- (43) Glendening, E. D. *J. Am. Chem. Soc.* **1996**, *118*, 2473–2482.
- (44) Glendening, E. D. *J. Phys. Chem. A* **2005**, *109*, 11936–11940.
- (45) Foster, J. P.; Weinhold, F. *J. Am. Chem. Soc.* **1980**, *102*, 7211–7218.
- (46) Reed, A. E.; Weinstock, R. B.; Weinhold, F. *J. Chem. Phys.* **1985**, *83*, 735–746.
- (47) Korchowiec, J.; Uchimaru, T. *J. Chem. Phys.* **2000**, *112*, 1623–1633.
- (48) Mayer, I. *Chem. Phys. Lett.* **2003**, *382*, 265–269.
- (49) Mayer, I.; Hamza, A. *Int. J. Quantum Chem.* **2005**, *103*, 798–807.
- (50) Szalewicz, K. *Wiley Interdiscip. Rev.: Comput. Mol. Sci.* **2012**, *2*, 254–272.
- (51) Jansen, G. *Wiley Interdiscip. Rev.: Comput. Mol. Sci.* **2014**, *4*, 127–144.
- (52) Jeziorski, B.; Moszynski, R.; Szalewicz, K. *Chem. Rev. (Washington, DC, U. S.)* **1994**, *94*, 1887–1930.
- (53) Vyboishchikov, S. F.; Salvador, P. *Chem. Phys. Lett.* **2006**, *430*, 204–209.
- (54) Krapp, A.; Bickelhaupt, F. M.; Frenking, G. *Chem. - Eur. J.* **2006**, *12*, 9196–9216.
- (55) von, H.; Moritz; Frenking, G. *Wiley Interdiscip. Rev.: Comput. Mol. Sci.* **2012**, *2*, 43–62.
- (56) Bader, R. F. W. *Acc. Chem. Res.* **1985**, *18*, 9–15.
- (57) Francisco, E.; Pendas, A. M.; Blanco, M. A. *J. Chem. Theory Comput.* **2006**, *2*, 90–102.
- (58) Wu, Q.; Ayers, P. W.; Zhang, Y. *J. Chem. Phys.* **2009**, *131*, 164112/1–164112/8.
- (59) Wu, Q. *J. Chem. Phys.* **2014**, *140*, 244109/1–244109/9.
- (60) Baba, T.; Takeuchi, M.; Nakai, H. *Chem. Phys. Lett.* **2006**, *424*, 193–198.
- (61) Nakai, H.; Kurabayashi, Y.; Katouda, M.; Atsumi, T. *Chem. Phys. Lett.* **2007**, *438*, 132–138.
- (62) Liu, S. *J. Chem. Phys.* **2007**, *126*, 244103.
- (63) Khaliullin, R. Z.; Cobar, E. A.; Lochan, R. C.; Bell, A. T.; Head-Gordon, M. *J. Phys. Chem. A* **2007**, *111*, 8753–8765.
- (64) Horn, P. R.; Sundstrom, E. J.; Baker, T. A.; Head-Gordon, M. *J. Chem. Phys.* **2013**, *138*, 134119.
- (65) Mo, Y.; Bao, P.; Gao, J. *Phys. Chem. Chem. Phys.* **2011**, *13*, 6760–6775.
- (66) Szabo, A.; Ostlund, N. S. *Modern Quantum Chemistry*; Dover Publications, Inc.: New York, 1996.
- (67) Colonna, F.; Savin, A. *J. Chem. Phys.* **1999**, *110*, 2828–2835.
- (68) Teale, A. M.; Coriani, S.; Helgaker, T. *J. Chem. Phys.* **2010**, *132*, 164115/1–164115/19.
- (69) Ryabinkin, I. G.; Kohut, S. V.; Staroverov, V. N. *Phys. Rev. Lett.* **2015**, *115*, 1–5.
- (70) Cuevas-Saavedra, R.; Ayers, P. W.; Staroverov, V. N. *J. Chem. Phys.* **2015**, *143*, 244116/1–244116/9.
- (71) Tsuneda, T.; Song, J.-W.; Suzuki, S.; Hirao, K. *J. Chem. Phys.* **2010**, *133*, 174101.
- (72) Salzner, U.; Baer, R. *J. Chem. Phys.* **2009**, *131*, 231101.
- (73) Iikura, H.; Tsuneda, T.; Yanai, T.; Hirao, K. *J. Chem. Phys.* **2001**, *115*, 3540–3544.
- (74) Kuemmel, S.; Kronik, L. *Rev. Mod. Phys.* **2008**, *80*, 3–60.
- (75) Gritsenko, O. V.; Baerends, E. J. *J. Chem. Phys.* **2002**, *117*, 9154–9159.
- (76) Chong, D. P.; Gritsenko, O. V.; Baerends, E. J. *J. Chem. Phys.* **2002**, *116*, 1760–1772.
- (77) Kraisler, E.; Kronik, L. *J. Chem. Phys.* **2014**, *140*, 18A540.
- (78) Schmidt, T.; Kraisler, E.; Kronik, L.; Kuemmel, S. *Phys. Chem. Chem. Phys.* **2014**, *16*, 14357–14367.
- (79) Stowasser, R.; Hoffmann, R. *J. Am. Chem. Soc.* **1999**, *121*, 3414–3420.
- (80) Janak, J. F. *Phys. Rev. B: Condens. Matter Mater. Phys.* **1978**, *18*, 7165–7168.
- (81) Ryabinkin, I. G.; Staroverov, V. N. *J. Chem. Phys.* **2014**, *141*, 084107.
- (82) Harrison, J. F.; Lawson, D. B. *J. Chem. Educ.* **2005**, *82*, 1205–1209.
- (83) Shaik, S.; Danovich, D.; Wu, W.; Hiberty, P. C. *Nat. Chem.* **2009**, *1*, 443–449.
- (84) Peterson, K. A.; Woods, R. C. *J. Chem. Phys.* **1987**, *87*, 4409–4418.
- (85) Fantuzzi, F.; Cardozo, T. M.; Nascimento, M. A. C. *J. Phys. Chem. A* **2015**, *119*, 5335–5343.
- (86) Montgomery, J. A., Jr.; Frisch, M. J.; Ochterski, J. W.; Petersson, G. A. *J. Chem. Phys.* **2000**, *112*, 6532–6542.
- (87) Wilson, S. *Electron Correlation in Molecules*; Dover Publications, Inc.: Mineola, NY, 1984.
- (88) Purwanto, W.; Al-Saidi, W. A.; Krakauer, H.; Zhang, S. *J. Chem. Phys.* **2008**, *128*, 114309/1–114309/7.

- (89) Gordon, M. S.; Truhlar, D. G. *Theor. Chim. Acta* **1987**, *71*, 1–5.
- (90) Hijikata, K. *J. Chem. Phys.* **1961**, *34*, 221–231.
- (91) Barden, C. J.; Rienstra-Kiracofe, J. C.; Schaefer, H. F., III. *J. Chem. Phys.* **2000**, *113*, 690–700.
- (92) Vaisnys, J. R.; Zmuidzinis, J. S. *Appl. Phys. Lett.* **1978**, *32*, 152–153.
- (93) Struve, W. S.; Kitagawa, T.; Herschbach, D. R. *J. Chem. Phys.* **1971**, *54*, 2759–2761.
- (94) Neoh, S. K.; Herschbach, D. R. *J. Chem. Phys.* **1975**, *63*, 1030–1032.
- (95) Housden, M. P.; Pyper, N. C. *Mol. Phys.* **2007**, *105*, 2353–2361.
- (96) Roki, F.-Z.; Ohnet, M.-N.; Fillet, S.; Chatillon, C.; Nuta, I. *J. Chem. Thermodyn.* **2014**, *70*, 46–72.
- (97) Kendall, R. A.; Dunning, T. H., Jr.; Harrison, R. J. *J. Chem. Phys.* **1992**, *96*, 6796–6806.
- (98) Balabanov, N. B.; Peterson, K. A. *J. Chem. Phys.* **2005**, *123*, 064107.
- (99) Douglas, M.; Kroll, N. M. *Ann. Phys. (Amsterdam, Neth.)* **1974**, *82*, 89–155.
- (100) Hess, B. A. *Phys. Rev. A: At., Mol., Opt. Phys.* **1985**, *32*, 756–763.
- (101) Hess, B. A. *Phys. Rev. A: At., Mol., Opt. Phys.* **1986**, *33*, 3742–3748.
- (102) Barysz, M.; Sadlej, A. J. *J. Mol. Struct.: THEOCHEM* **2001**, *573*, 181–200.
- (103) de, J. W. A.; Harrison, R. J.; Dixon, D. A. *J. Chem. Phys.* **2001**, *114*, 48–53.
- (104) Ceolin, G. A.; Berredo, R. C.; Jorge, F. E. *Theor. Chem. Acc.* **2013**, *132*, 1–13.
- (105) Jorge, F. E.; Canal Neto, A.; Camiletti, G. G.; Machado, S. F. *J. Chem. Phys.* **2009**, *130*, 064108.
- (106) Marenich, A. V.; Cramer, C. J.; Truhlar, D. G. *J. Phys. Chem. B* **2009**, *113*, 6378–6396.
- (107) O'Boyle, N. M.; Tenderholt, A. L.; Langner, K. M. *J. Comput. Chem.* **2008**, *29*, 839–845.